DOPAMINE TOXICITY AND OXIDATIVE STRESS IN ZEBRAFISH LARVAE AS A MODEL OF PARKINSON'S DISEASE NEUROPATHOLOGY

By

Sarah Josephine Stednitz

A Thesis Presented to

The Faculty of Humboldt State University

In Partial Fulfillment of the Requirements for the Degree

Master of Arts in Psychology: Academic Research

Committee Membership

Dr. Ethan Gahtan, Committee Chair

Dr. Christopher Aberson, Committee Member

Dr. Bruce O'Gara, Committee Member

Dr. Christopher Aberson, Graduate Coordinator

May, 2014

Abstract

DOPAMINE TOXICITY AND OXIDATIVE STRESS IN ZEBRAFISH LARVAE AS A MODEL OF PARKINSON'S DISEASE NEUROPATHOLOGY

Sarah Josephine Stednitz

Dopamine signaling is conserved across all animal species and has been implicated in the disease process of many neurological disorders, including Parkinson's disease (PD). The primary neuropathology in PD involves the death of dopaminergic cells in the substantia nigra (SN), an anatomical region of the brain implicated in dopamine production and voluntary motor control. Increasing evidence suggests that the neurotransmitter dopamine may have a neurotoxic metabolic product (DOPAL) that selectively damages dopaminergic cells. This study was designed to test this theory of oxidative damage in an animal model of Parkinson's disease, using a transgenic strain of zebrafish with fluorescent labeling of cells that express the dopamine transporter. The pretectum and ventral diencephalon exhibited reductions in cell numbers and fluorescence intensity due to L-DOPA treatment, and this was partially rescued by MAO inhibition. Consistent with the MPTP model of PD in zebrafish larvae, spontaneous locomotor behavior in L-DOPA treated animals was depressed following a 24-hour recovery period, while visually-evoked startle response rates and latencies were unaffected.

Table of Contents

List of Figures

List of Tables

Table Page

Dopamine Toxicity and Oxidative Stress in Zebrafish Larvae and their Applications in PD Research

Parkinson's disease (PD) is a neurodegenerative disorder characterized by tremor and disruptions to voluntary movement. The disorder primarily affects people age 50 and older, and the prevalence and risk of developing sporadic PD increases substantially with age (de Lau & Breteler, 2006). Although PD is best known for its motor symptoms, disruption of emotional regulation and other cognitive functions is common.

The primary neuropathology in PD involves the death of dopaminergic cells in the pars compacta of the substantia nigra (SN), an anatomical region of the brain implicated in dopamine (DA) production and voluntary motor control. Fearnley and Lees (1991) found neural loss in the SN increases with age in PD, consistent with a worsening prognosis and increased symptom severity in older patients. The SN is considered part of a larger structure known as the basal ganglia; neural circuits in the basal ganglia, in particular the nigrostriatal pathway, appear to be crucial to the successful execution of both innate and learned motor behaviors (Groenewegen, 2003). The motor disturbances typical of PD are theorized to be a result of damage to this nigrostriatal pathway.

Traditional treatments for PD are designed to increase dopamine availability or receptor stimulation and have not been demonstrated to slow the progression of neurodegeneration. As a result, treatment has focused primarily on ameliorating symptoms rather than targeting the underlying mechanism. The most common treatment for PD is L-DOPA, a metabolic precursor of DA that is able to pass the blood-brain barrier. L-DOPA partially compensates for the loss of DA-producing cells in the SN by increasing synaptic DA concentrations, but does not address

any factors that may have caused the initial neurodegeneration. A more recent treatment approach, deep brain stimulation, improves symptoms by electrically exciting neurons in these and related brain areas (Bronstein et al., 2011), but pharmacological interventions like L-DOPA still represent the most common Parkinson's treatment.

As PD progresses and more neurons are lost (Fearnley & Lees, 1991), increasing quantities of L-DOPA must be administered in order to maintain the same level of therapeutic effect, a strategy that increases adverse side effects and eventually loses effectiveness altogether. Directly augmenting DA concentrations via L-DOPA has also been associated with worsening impulse control and an increased tendency to form addictive behaviors (Merims & Giladi, 2008). Such side effects reflect the fact that DA influences multiple functional systems in the brain, including the reinforcement learning system, and not just voluntary motor control (Figure 1).

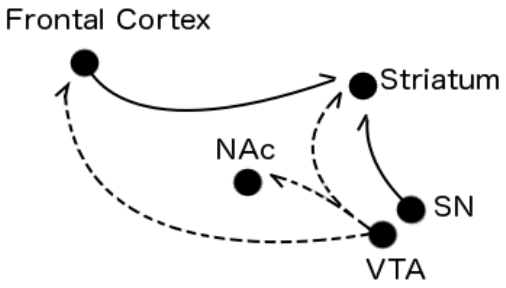

Figure 1. A schematic of dopaminergic pathways and associated functions in the human brain. Dotted lines represent the mesolimbocortical pathway involved in reinforcement learning. Solid lines represent the mesostriatal motor pathway involved in voluntary motor behavior. NAc: nucleus accumbens; SN: substantia nigra; VTA: ventral tegmental area.

These shortcomings of current treatments highlight the need for new therapies that slow the progression of PD, rather than compensating for decreased neurotransmitter concentrations. Monoamine oxidase inhibitors (MAOIs) are increasingly used as an adjunctive therapy (i.e.,

therapies given in addition to L-DOPA). MAOIs act by preventing DA metabolism, simultaneously increasing DA availability and preventing the formation of potentially toxic metabolites. A growing body of evidence implicates these DA metabolites as a potential cause for neuron death in PD (Burke et al., 2004; Goldstein et al., 2013; Goldstein, Sullivan, Holmes, Kopin, Basile, & Mash, 2011; Li, Lin, Minteer, & Burke, 2001; Panneton, Kumar, Gan, Burke, & Galvin, 2010).

The specific enzymatic pathways of DA metabolism are highly conserved across model animal species. Using model animals provides an opportunity to precisely manipulate contributing factors and examine the disease process in ways that are not possible with human PD patients. Zebrafish (*Danio rerio*) are used extensively for neurotoxicity and genetics studies due to the ease of studying behavior and visualizing neurons in vivo. Understanding the effects of DA metabolites in otherwise healthy zebrafish larvae may yield new insight into the etiology and treatment of PD.

Literature Review

Theories of Parkinson's Neuropathology

Neurodegeneration observed in PD is highly selective to dopaminergic neurons found in the SN. Research has focused on the qualities unique to these neurons that may render them especially vulnerable to the disease process. The affected cells are notable for their expression of the dopamine transporter (DAT), a transmembrane protein that is responsible for the reuptake of DA in presynaptic neurons. Cell death in PD appears to primarily affect the neurons that express this transporter protein, and increased DAT expression results in greater vulnerability to cell death (Burke et al., 2004). This is seen in the resilience to dopaminergic toxins of DA neurons in the mesocortical pathway, which show comparatively little DAT expression.

Treatment with L-DOPA fails to slow the rate of neurodegeneration in PD, suggesting that a lack of DA receptor stimulation alone is not responsible for the observed cell death. MAOIs, which act by preventing the metabolism of DA, represent a promising class of drugs that alter underlying biochemical processes rather than directly targeting synaptic transmission. The MAOI rasagiline has been shown to reduce the severity and duration of motor symptoms in multiple long-term clinical trials (Rascol et al., 2005; Rascol et al., 2011; Parkinson Study Group, 2005; Olanow et al., 2009). In one such trial (the ADAGIO study), the long-term effects of rasagiline in PD were examined in order to determine if the drug influenced disease progression (Rascol et al., 2011). Utilizing a delayed-start design, patients were randomly assigned to an early-start group (receiving rasagiline for 72 weeks) or a delayed-start group (receiving a placebo for the first 36 weeks and rasagiline for the subsequent 36 weeks). Motor symptoms were improved in both treatment groups relative to placebo, but notably patients in the

early-start condition exhibited a decreased need for additional antiparkinsonian therapy compared to those in the delayed-start condition.

These findings suggest that MAOIs have two potential therapeutic mechanisms: providing acute symptomatic relief by increasing dopamine availability, and slowing the long-term progression of the disease by inhibiting dopamine metabolism. Because the ADAGIO study included many subjects who had been recently diagnosed with PD, it is possible that these effects would not be replicated in patients with more advanced forms of the disease (Antonini, 2011). Nevertheless, MAOIs are a promising therapy for PD and clinical trials continue to be conducted to determine its efficacy and tolerability in a wider range of patients. Studies with animal models are a necessary complement to these trials, in order to elucidate the mechanism of their therapeutic effects.

Humans possess two distinct MAO variants: MAO-A, located on the outer membrane of mitochondria within the neuron, and MAO-B, located within astrocytes (Burke et al., 2004). Inhibition of either MAO isoform results in greater quantities of circulating DA by slowing the rate of its degradation. Inhibitors of the A isoform are no longer commonly prescribed due to the increased risk of adverse effects such as hypertension and tyramine sensitivity, and as such only MAO-B inhibitors are used in the treatment of PD. Age-related increases in glial cell numbers and MAO-B enzymatic activity is encouraging, because it suggests that inhibiting the B isoform will be an even more potent therapy in the population most affected by PD (Fowler et al., 1997; Saura et al., 1997).

The Oxidative Damage Hypothesis and Potential Neurotoxic Role of Dopamine Metabolites

Given their role in catecholamine metabolism, MAOIs have additional therapeutic potential aside from merely maintaining sufficient synaptic DA concentrations. As an oxidative enzyme, MAO produces unstable metabolic byproducts that generate reactive oxygen species (ROS). ROS are oxygen-containing molecules of high thermodynamic energy and low stability, qualities that render them highly reactive. Dopamine is metabolized by MAO to L-3,4-dihydroxyphenylalanine (DOPAL), the aldehyde form of DA that reacts with hydrogen peroxide (H_2O_2) to form ROS (Li, et al., 2001). Under normal conditions, DOPAL is rapidly converted to DOPAC (a harmless acid derivative of DOPAL) by aldehyde dehydrogenase, but this mechanism appears to be disrupted in PD (Figure 2).

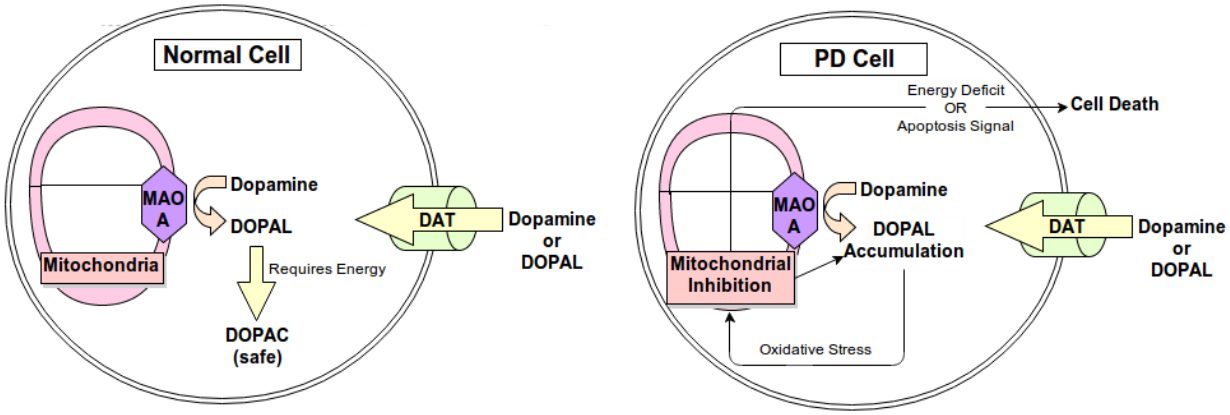

Figure 2. Dopamine metabolism in normal and PD dopaminergic cells. Under normal conditions, DA is metabolized to DOPAL, which is then converted to DOPAC, its harmless acid derivative. In PD, DOPAC production is decreased, resulting in increased DOPAL production.

DA and its metabolites all show reduced levels in human PD patients relative to healthy controls due to the decrease in DA production. However, the DOPAL:DA and DOPAL:DOPAC ratios are elevated in PD (Goldstein et al., 2013). DOPAL:DOPAC ratios in PD brains have been

reported to be as high as 3.4 times that of healthy age-matched adults (Goldstein et al., 2011). The increased quantities of DOPAL relative to other molecules indicates a failure to convert DOPAL into its benign form (DOPAC) in PD. The DA/DOPAL condensation product tetrahydropapaveroline (THP) has also been identified in the brains of PD patients (McQueen, 2010). Though this may primarily be a result of the L-DOPA treatment patients received rather than any pre-existing pathological process, the presence of THP also implies a failure to convert DOPAL into its less reactive metabolite.

The oxidative damage hypothesis of PD states that DOPAL damages dopaminergic cells by reacting with H_2O_2 (itself a byproduct of DA metabolism), forming ROS that inhibit mitochondrial function (Burke et al., 2004). Previous studies have directly demonstrated the neurotoxicity of DOPAL produced during normal DA metabolism. Burke et al. (2004) examined the toxicity of potentially reactive catecholamine metabolites in adult rats. Following direct injection of 50-750 ng DOPAL in the rat SN, dose-dependent dopaminergic cell death was observed. As little as 100 ng DOPAL was sufficient to cause loss of dopaminergic neurons in the SN, while the ventral tegmental area (VTA) was comparatively unaffected. This discrepancy can be accounted for by the differential expression of the DAT in the two areas, as the SN has greater DAT expression than the VTA. No similar effect was found with 500 ng DA, or other DA metabolites such as DOPAC, implicating DOPAL as the sole neurotoxic metabolite. Burke et al. (2004) also found that DOPAL generates ROS under conditions of oxidative stress where DA and its other metabolites do not, in concordance with previous research by Li et al. (2001). Given that DOPAL-induced cell death is correlated to the relative degree of DAT expression in these brain regions, it is likely that DOPAL enters the cell through the DAT (Burke et al., 2004), and

exerts its damage intracellularly. DOPAL can also be produced intracellularly by mitochondrial MAO-A (Goldstein et al., 2013), but DOPAL produced by MAO-B activity and entering through the DAT is likely the larger source of intracellular DOPAC after synaptic release of dopamine.

The toxicity of metabolic compounds produced by MAO has been demonstrated in studies of the neurotoxin, 1-methyl-4-phenyl-1,2,3,6-tetrahydropyridine (MPTP). In a now-infamous case from 1982, MPTP was produced accidentally during the manufacture of an opioid analgesic, Desmethylprodine (MPPP). Several users of the contaminated drug rapidly developed a movement disorder indistinguishable from PD (Langston & Palfreman, 1996). The specific mechanism of MPTP toxicity has since been elucidated. MPTP is metabolized by MAO-B to form MPP+, a molecule capable of generating ROS that inhibit mitochondrial function. MPP+ enters the cell through the DAT and thus selectively damages dopaminergic cells, resulting in the characteristic motor symptoms. Cells can be rescued by simultaneous administration of MAOIs, preventing the conversion of MPTP into MPP+, or by blocking the DAT and preventing entrance of MPP+ into the cell (Xi et al., 2011). Although MPTP is far more reactive than DA or its metabolites, its mechanism provides support for the hypothesis that MAO's products cause cell death by ROS-induced mitochondrial inhibition. Similarly, cells must express the DAT to be vulnerable to this toxicity. The idea that MAO mediates neuronal damage in PD is also supported by surprising finding that cigarette smokers are less likely than nonsmokers to develop PD (Castagnoli & Murugesan, 2004). Cigarette smoking is known to inhibit MAO-B activity in the brain (Fowler et al., 2008), theoretically preventing the production of toxic metabolites.

Further support for the oxidative damage hypothesis stems from hereditary autosomal mutations identified in some PD patients. Mutations in the gene *PINK1* have been identified as the cause of one form of early-onset PD. The PINK1 protein is theorized to mitigate intracellular oxidative damage, in part by preventing premature cell death (Pridgeon, Olzmann, Chin, & Li, 2007). Temporary suppression of the *PINK1* gene in zebrafish causes neurodegeneration, increased ROS concentrations, and reduced locomotor activity (Anichtchik et al., 2008; Xi et al., 2010). Although individuals with this mutation represent the minority of PD patients, it reinforces the importance of regulating oxidative stress in Parkinsonian pathogenesis.

Additional support for the critical role of mitochondria in DA-related neurotoxicity is found in the effects of *parkin*, a gene associated with hereditary PD (Kitada et al., 1998). The function of the parkin protein is currently unknown, but transgenic animal knockouts exhibit symptoms that mirror the effects of the mutation in humans. Transgenic *parkin* knockout zebrafish exhibit dopaminergic cell death and decreased complex I mitochondrial activity in the surviving cells (Flinn et al., 2009), both hallmarks of PD in humans. This dopaminergic cell death occurs primarily in the ascending dopaminergic neurons of the posterior tuberculum, a structure proposed to be homologous to the human SN. The magnitude of cell death was increased by administration of MPTP, providing additional support for the role of oxidative stress vulnerability in PD pathogenesis.

Zebrafish Models in Parkinson's Research

Owing to their small size and predictability of certain behaviors, zebrafish are a useful animal for correlating behaviors with physiological phenotypes. A great deal of genetic and molecular information is available from previous research. The larvae are transparent, allowing

for excellent visibility of internal brain structures compared to other model animals. The ease of breeding zebrafish and their rapid neural development allows for high throughput experiments. Dozens of larval zebrafish can be imaged simultaneously over extended periods of development, and their behavior reliably and automatically quantified using image analysis software.

The biochemical processes previously discussed are conserved from mouse models to zebrafish. Like their mammalian counterparts, suppression of *PINK1* gene expression (knockdown) in larval zebrafish decreases locomotor activity (Xi et al., 2010). Furthermore, Anichtchik et al. (2008) reported *PINK1* knockdown zebrafish had increased ROS concentrations, loss of neurons associated with motor control, and disrupted mitochondrial function. Similarly, MPTP toxicity causes motor deficits and dopaminergic cell death in zebrafish, and this toxicity can be abolished by co-administration of MAO-B inhibitors or DAT antagonists (McKinley et al., 2005; Lam, Korzh, & Strahl, 2005; Xi et al., 2011). This neuronal death has been demonstrated in ventral diencephalon (vDC), a cluster of DAT-expressing neurons that appear homologous in function and neurochemistry to dopaminergic motor circuits in mammals (Xi et al., 2011).

Dopamine neurotransmission and its role in motor control is evolutionarily ancient and present in all animal species, even invertebrates. Mammals evolved novel dopaminergic brain structures and pathways, including the nigrostriatal pathway that is damaged in PD. These evolutionarily recent structures complicate the use of non-mammalian vertebrates to model PD. However, it has been proposed that the zebrafish vDC is homologous to the A11 system in mammals, an area involved in motor control and anatomically associated with the nigrostriatal DA system (Schweitzer, Lohr, Filippi, & Driever, 2012). Parkin-deficient zebrafish also exhibit

cell death in the vDC, reinforcing the relevance of this location to zebrafish models of PD (Flinn et al., 2009).

The dopaminergic posterior tubercular neurons in zebrafish (groups DC2 and DC4) send ascending projections from the vDC into the subpallium, a region involved in motor control in both fish and mammalian brains (Schweitzer et al., 2012; Tay, Ronneberger, Ryu, Nitschke, & Driever, 2011). These vDC neurons have been theorized as the primary source of DA for spontaneous motor behaviors in fish. The zebrafish vDC has also been demonstrated to be susceptible to MPTP injury (Lam, Korzh, & Strahl, 2005; Xi et al., 2011). Taken together, these findings suggest that mechanisms of DA cell death in the zebrafish vDC and in human nigrostriatal neurons are sufficiently related to investigate PD-related neurodegenerative processes in the zebrafish.

Zebrafish larvae exhibit spontaneous locomotor activity, engaging in brief bouts of swimming in the absence of any stimulation. Deficits in spontaneous activity have been used previously in high-throughput behavioral screens for neurotoxicity (Muto et al., 2005; Selderslaghs, Hooyberghs, De Coen, & Witters, 2010). Dopaminergic cell death has also been correlated with reduced locomotor activity in zebrafish larvae (McKinley et al., 2005; Xi et al., 2010; Xi et al., 2011). Spontaneous swimming activity can therefore be used as a metric for the health of the dopaminergic motor system in larval zebrafish.

In addition to spontaneous swimming bouts, zebrafish larvae exhibit a number of reflex behaviors related to predator avoidance, including a well-characterized escape or startle swim that can be elicited with an appropriate visual, tactile, auditory or vestibular stimulus. The visually-evoked startle response has been hypothesized to be an evolved response to shadows

cast by predatory fish (Portugues & Engert, 2009). This behavior is theorized to be controlled by reticulospinal circuits, and can be elicited reliably with highly consistent temporal and kinematic features (short latency and high angle initial body bend). These factors render it a suitable behavioral index of sensorimotor functioning independent of spontaneous locomotor activity (Kimmel, Patterson, & Kimmel, 1974).

Statement of the Problem

This research was designed to test three primary questions:

1. Can L-DOPA, a drug that augments DA levels in the brain, be toxic to DA neurons and inhibit related behaviors?

2. Assuming evidence of L-DOPA toxicity is found, is it associated with markers of oxidative stress?

3. Can inhibitors of DA metabolism prevent oxidative stress and neurobehavioral toxicity of L-DOPA?

These questions are important because they may support the theory that there are unintended negative effects of L-DOPA, the primary therapeutic drug for PD. These experiments were performed in zebrafish larvae, utilizing a transgenic zebrafish line (*dat:eGFP*) in which all cells expressing the DAT are fluorescent and easily visualized with a fluorescence microscope (Xi et al., 2011). Using larval zebrafish also made it feasible to test a large enough sample to achieve sufficient statistical power. Test larvae were treated with L-DOPA, or L-DOPA together with a MAOI, using bath application. Neurotoxicity was assessed by comparing fluorescent dopamine neurons in the pretectum and ventral diencephalon between treated and control larvae, and by comparing locomotor and startle behaviors across the same groups. I predicted that cell numbers and behavioral function would decrease after L-DOPA treatment but be unaffected when a MAOI is administered simultaneously. I predict that markers of oxidative stress will be correlated with the degree of neurotoxicity and behavioral impairment and I plan to test this by analyzing oxidative stress markers in each drug treatment group using an immunoassay. This is

an important test of the theoretical mechanism of L-DOPA induced toxicity. However, this experiment could not be completed in time for presentation in this thesis so it is not included as a hypothesis.

The selectivity of the fluorescence expression to dopaminergic neurons in *dat:eGFP* zebrafish has been validated by simultaneous immunolabeling of tyrosine hydroxylase, an enzyme used in dopamine synthesis and a common marker of dopaminergic neurons (Xi et al., 2011). Specifically, the dopaminergic cell groups DC2 and DC4 of the vDC that project into the subpallium are tyrosine hydroxylase-positive and labeled with transgenic fluorescence expression. While no direct homolog to the human substantia nigra has been found in zebrafish, existing evidence supports targeting the zebrafish vDC as a functionally similar structure (Flinn et al., 2009; Schweitzer, Lohr, Filippi, & Driever, 2012; Tay et al., 2011; Xi et al., 2011). Numerous studies have been published on dopaminergic motor systems and related disorders using zebrafish, but to my knowledge this was the first study in zebrafish to address toxicity from DA and its metabolites.

Hypotheses

Hypothesis 1a. Bath application of L-DOPA for 24 hours in 5 dpf zebrafish larvae will reduce the number of fluorescent neurons in the pretectum measured 48 hours later using fluorescence microscopy.

Hypothesis 1b. Bath application of L-DOPA for 24 hours in 4 dpf zebrafish larvae will reduce the fluorescence intensity in the ventral diencephalon measured 24 hours later using fluorescence microscopy.

Rationale for Hypothesis 1. L-DOPA treatment will result in elevated dopamine concentrations in the brain, which will in turn increase the levels of dopamine metabolites with potentially harmful oxidative properties.

Hypothesis 2. MAOI administration will prevent dopaminergic cell loss and damage caused by L-DOPA treatment in the pretectum and vDC of zebrafish larvae.

Rationale for Hypothesis 2. MAOIs prevent the degradation of dopamine into its reactive metabolite, DOPAL, which has been demonstrated to have neurotoxic effects. Zebrafish larvae are vulnerable to MPTP damage in the vDC by a similar theoretical mechanism of oxidative stress, and this damage can be mitigated by co-administration of MAOIs.

Hypothesis 3. Spontaneous locomotor behaviors will be reduced as dopaminergic cell loss increases, while startle response rate and latency will be unaffected.

Rationale for Hypothesis 3. Dopaminergic cell loss reduces spontaneous locomotor activity in zebrafish larvae. Since this cell loss hypothetically affects neural circuits responsible for spontaneous locomotor activity, sensorimotor reflexes are not expected to be disrupted.

Method

Instruments and software

Behavioral data were obtained with a PTEM Photon Focus high speed camera and Pixelink time lapse camera, with capture signals and sensory stimuli delivered by a LabJack controller programmed with DAQFactory. Images were analyzed using custom scripts (Appendix A) for ImageJ (NIH) and data were analyzed with R version 3.0.0. Fluorescence images were obtained with an Olympus Fluoview FV1000 confocal microscope using a 20X water immersion lens.

Subjects

A clutch of approximately 50 zebrafish (*Danio rerio*) embryos stably expressing the *dat:eGFP* transgene was obtained from the University of Ottawa and raised to adulthood to form a breeding colony for these experiments. The *dat:eGFP* strain was chosen because it exhibits fluorescent labeling of cells that express the DAT, allowing for easy identification of the target cell clusters and quantification of the cells within it. All preliminary experiments were performed as described in IACUC protocol number 12/13.P.88-A. All adult DAT fish were maintained in the breeding colony and experiments utilized larvae between ages 5-8 days old.

Experimental design and drug treatments

Larvae were housed in standard egg water (0.25 g instant ocean, 0.075 g calcium sulfate, 0.1 mL methylene blue per L water), and all drugs were dissolved in this solution. The two treatment drugs used were 3,4-Dihydroxy-L-phenylalanine ethyl ester (Levodopa ethyl-ester, abbreviated L-DOPA) and (R)-N-methyl-N-(1-phenylpropan-2-yl)prop-1-yn-3-amine

(Selegiline). The ethyl ester form of L-DOPA was used because of its stability in alkaline solution (zebrafish water is approximately pH 7.2). Ethyl 3-aminobenzoate methanesulfonate (MS-222) was used as an anesthetic to immobilize larvae during imaging.

At 5 days post fertilization (dpf), larvae were randomly assigned to one of three conditions, consisting of at least 20 larvae each. Previous research on the vDC in this strain of zebrafish (n = 18) found MPTP toxicity reduced cell populations from the control average of 49.8 ± 3.9 cells to 38.9 ± 6.1 cells, yielding an effect size of d = 2.13 (Xi et al., 2011). Preliminary manual cell counts of pretectal cell populations in healthy 6 dpf zebrafish for the current study (n = 20) found an average cell number of 56.67 ± 9.89. Given that the MAOI treatment group was not expected to differ from controls, a power analysis was performed with the intent of achieving sufficient sample sizes to detect differences between L-DOPA treated and control larvae. Assuming a pooled standard deviation of 9.89 and an average reduction of 6 cells in L-DOPA treated larvae relative to controls (d = 0.6), group sizes of 20 (n = 60 total) were determined to be sufficient to achieve a statistical power of .85.

All solutions were mixed in standard pH 7.2 egg water. The control group was housed in pH-matched egg water. Experimental fish were given L-DOPA or L-DOPA along with the MAOI, selegiline (hereafter referred to as MAOI). Dosages for each condition are provided in Table 1. Larvae were left in their respective solutions for 24 hours, then removed from the drug and placed into recovery dishes containing egg water.

Due to variable success in breeding of adult DAT zebrafish, experiments had to be repeated using different clutches until sufficient sample sizes were obtained. Larvae from each

clutch were always randomly assigned to the three comparison groups to distribute variability across clutches.

Table 1.
Experimental design and drug dosages for all three groups

	L-DOPA Dosage	**MAOI Dosage**
Group 1 (Control)	N/A	N/A
Group 2 (L-DOPA)	1 mM	N/A
Group 3 (L-DOPA +MAOI)	1 mM	100 μM

Behavior

Larvae at age 6 dpf were transferred with a plastic pipette into individual 10 mm wells containing 4 mL of egg water. Spontaneous locomotor activity was measured over a 6 hour period for each fish in all groups. Time lapse images were taken at 1:00 PM at a rate of 1 Hz for ten minutes. To quantify locomotor activity, each image in the video was subtracted from the previous image, resulting in a new video in which pixels were visible only if their intensity had changed from one frame to the next, which should occur only when the fish moved. The particle counting function in ImageJ was then used to determine the percentage of video frames, and therefore the percentage of time, that each fish spent in motion during the recording period (Figure 3). A subset of larvae (n = 48) underwent an additional behavioral recording session on the next day (7 dpf) to determine whether any drug effects on behavior changed over time, potentially tracking the accumulation of neurotoxic effects.

The visually-evoked startle response was also measured with the use of a high-speed camera capturing video at 60 frames per second. Dimming was achieved by illuminating a standard 20 watt fluorescent light bulb 10 inches above the recording plate (producing even

illumination of the plate), and suddenly extinguishing the light during the bouts of high speed video capture. The camera imaged the recording plate from below. A visible light blocking filter was placed in front of the camera lens and an infrared lamp was used to illuminate the scene for camera. This setup allowed the stimulus light to be turned on and off without affecting the recorded image, and for the dimming-evoked startle movements to be imagined in the dark. Both the startle light and the camera were controlled by a custom computer script that allowed precise timing of the experimental events. Recorded video images were analyzed to measure whether a startle response occurred (defined as movement of more than 5 pixels within 2 seconds after light dimming) response rates and the latency of movement onset for each fish Light dimming trials were presented 30 minutes after spontaneous activity recording and the light remained off for 60 seconds.

Acute drug effects on behavior were analyzed via ANOVA using R version 2.15.2. Drug effects on behavior over time were analyzed using a mixed-model repeated measures ANOVA with drug treatment as the between subjects variable and locomotor activity and startle latency as within subjects variables.

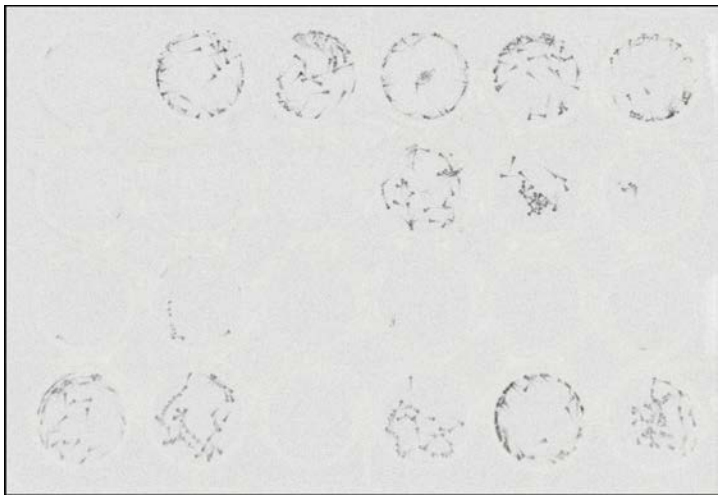

Figure 3. Composite time-lapse image of zebrafish larvae in a standard 24-well plate exhibiting spontaneous locomotor activity over a ten minute period. The image series was processed with successive subtraction and Z projection using ImageJ. Black dots indicate the location of larva within a well.

Dopaminergic cell populations

Confocal images of GFP+ pretectal neurons were acquired by imaging a consistent volume of tissue (100µm height x 100µm length x 40µm depth) positioned so that the entire pretectum bilaterally was captured within the imaged volume. Pretectal cell populations were quantified by counting the total number of GFP+ cells within the imaged volume. This volume was standardized by manually determining the center point of the pretectal cell cluster, then extending 20 microns above and below and 50 microns laterally from this center (Figure 4). This required a series of images through the depth plane, which is acquired automatically by the confocal system controls by moving the objective lens a consistent distance (1.5µm in this case) after each image. Preliminary experiments indicated this imaged volume is sufficient to contain the entire pretectum while excluding cells belonging to other structures. The soma of individual cells were manually labeled for each image in the stack by a rater blind to the group assignments. Labeled cells were then counted using the ImageJ 3D Object Counter plugin for ImageJ (Figure 5). Decreases in cell numbers relative to the control population were interpreted as cell loss. As imaging is a time-consuming process, not every larva tested in behavioral assays was imaged. Instead, subsets of 20 larvae from each group were randomly selected for imaging at 7 dpf. Cell counts were analyzed via ANOVA using R version 2.15.2.

Neurons within the vDC were also tested for L-DOPA neurotoxicity. Although all DAT expressing cells should be vulnerable to this mechanism of neurotoxicity, the vDC is arguably the most relevant anatomical structure in zebrafish for modeling PD because it is the putative

homolog of the mammalian substantia nigra. The vDC was imaged both before and after drug treatment, and GFP expression was assessed as a within subjects factor, which is in contrast to the pretectum experiment in which neurons were imaged only once after the drug treatment. The purpose of analyzing changes in GFP intensity within larvae was to remove the effect of individual differences in baseline GFP expression and to detect changes in fluorescence intensity level rather than just changes in the number of neurons counted. Confocal images of GFP+ vDC neurons were acquired by imaging a consistent volume of tissue (200µm height x 200µm length x 40µm depth) positioned so that the entire vDC was captured within the imaged volume. (Figure 6). The average fluorescence intensity through the imaged volume that captured the vDC was calculated and compared between pre-drug and post-drug imaging sessions. These change in fluorescence values were analyzed by ANOVA using R version 2.15.2.

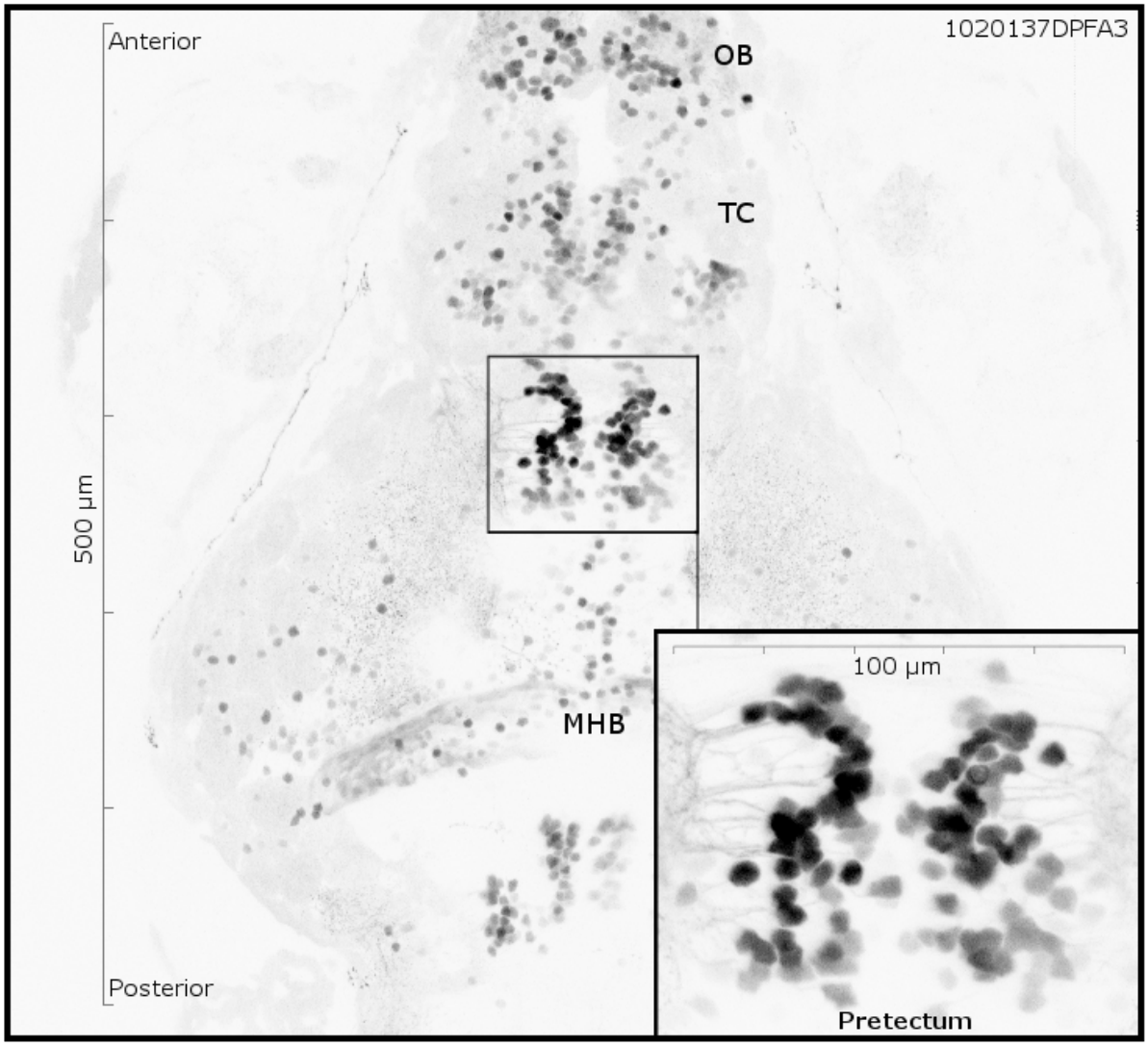

Figure 4. Fluorescence image of dopamine transporter expressing cells in the zebrafish brain, with the pretectum inset to show the size of the voxel and resolution of images to be used in cell counting. OB: olfactory bulb; TC: telencephalon; MHB: midbrain-hindbrain boundary. Image acquired by Sarah Stednitz.

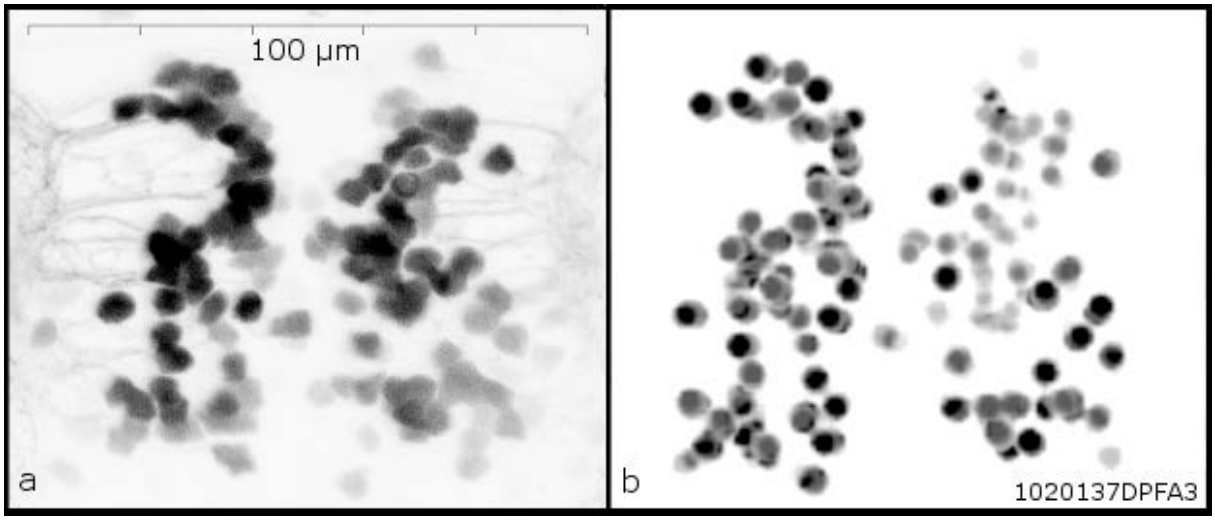

Figure 5. a: Unedited fluorescence image of dopamine transporter expressing cells in the pretectum. b: 3D reconstruction of manually labeled tectal cells created with the 3D Object Counter plugin, written for ImageJ by Fabrice Cordelieres & Jonathan Jackson. Image acquired by Sarah Stednitz.

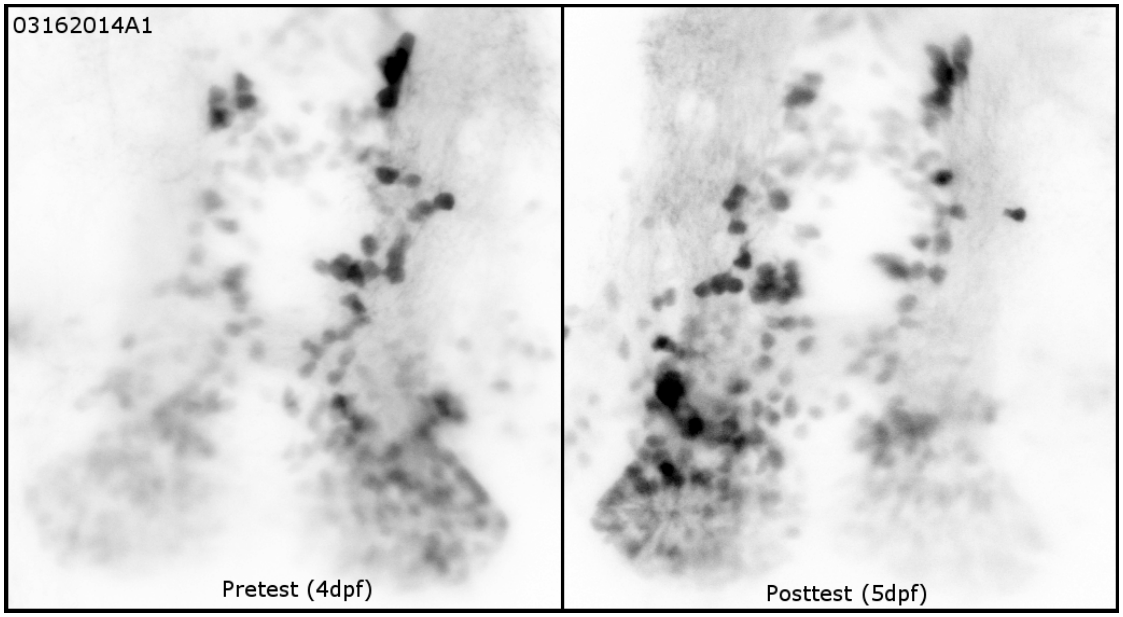

Figure 6. Summed fluorescence image of dopamine transporter expressing cells in the ventral diencephalon (vDC) inset to show the size of the voxel (200 µm x 200 µm x 40 µm depth). The pictured larva was treated with L-DOPA for 24 hours and exhibited a 1.6% increase in fluorescence intensity. Images acquired by Sarah Stednitz.

Results

Behavior

Acute drug effects. Acute drug exposure affected locomotor activity in both drug treatment groups relative to controls, $F(2,163) = 10.326$, $p < .001$, partial $\eta^2 = .112$ (Table 2). Control fish ($n = 59$) were active for 30.5% of the recording duration on average. Consistent with prior research on acute exposure to dopaminergic agents (Irons, MacPhail, Hunter, & Padilla, 2010), larvae treated with L-DOPA ($n = 62$) exhibited locomotor hyperactivity and were active for 41.9% of the recording duration on average. Fish treated with both L-DOPA and an MAOI ($n = 45$) exhibited the hyperserotonergic phenotype previously described by Sallinen et al. (2009), and were active for only 17.8% of the recording duration on average (Figure 7).

Delayed drug effects. Given the pronounced effects from acute drug exposure, a repeated measures design was implemented to determine if locomotor activity would be impaired due to cell loss even after allowing for more time to recover from acute drug effects. A mixed model repeated measures ANOVA revealed a main effect for both treatment group and time post-exposure on locomotor activity, $F(2,45) = 20.925$, $p < .001$, partial $\eta^2 = .482$ and $F(1,45) = 40.655$, $p < .001$, partial $\eta^2 = .475$ respectively (Table 3, Figure 7). These main effects are qualified by an interaction between treatment group and time, $F(2,45) = 11.920$, $p < .001$, partial $\eta^2 = .346$. Simple effects tests revealed that L-DOPA treated fish became hypoactive relative to controls 24 hours after drug exposure, $F(1,45) = 55.306$, $p < .001$. MAOI treated fish did not recover from acute drug effects following the 24 hour recovery period ($F(1,45) < .001$, $p = .986$), consistent with previous research by Sallinen et al (2009).

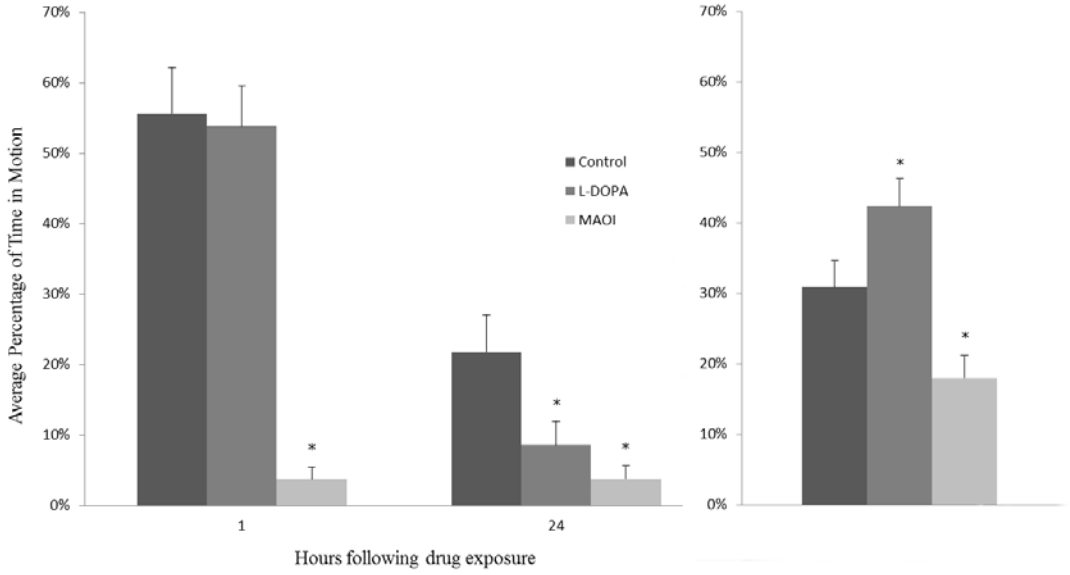

Figure 7. Left: Average percentage of time spent in motion for 6 and 7 dpf larvae by hours following drug exposure (n = 48). Right: Average percentage of time spent in motion for 6 dpf larvae immediately following drug exposure (n = 166). Error bars indicate s.e.m., and asterisks indicate groups that differ significantly from the control.

Startle response. Drug treatment did not influence the latency of visually-evoked startle responses in 6 and 7 dpf zebrafish larvae as determined by a mixed model repeated measures ANOVA, $F(1,18) = 1.309$, $p = .268$, partial $\eta^2 = .06$. Latency increased from 6 to 7 dpf regardless of treatment group, $F(1,18) = 31.731$, $p < .001$, partial $\eta^2 = .638$. No interaction was found between latency and group, $F(1,18) = 0.103$, $p = .752$, partial $\eta^2 = .006$. Due to the low response rate in the MAOI group (33.3%), it was not possible to statistically compare any changes in latency (a startle movement had to have occurred in order to calculate latency). Means and other statistics are reported in Table 2.

Only MAOI treatment influenced the probability of a visually-evoked startle response, $F(2,45) = 24.658$, $p < .001$, partial $\eta^2 = .523$. MAOI treated fish (n = 15) had a diminished likelihood of exhibiting the startle response (33.3%). L-DOPA treated fish (n = 21) had an

overall response rate of 80.9%, while control fish (n = 12) exhibited a 95.8% response rate, and the latter groups did not differ as determined by a post hoc Tukey test.

Table 2.
Means, standard deviations, and relevant statistics for all behavioral experiments performed.

Experiment	**L-DOPA**	**L-DOPA & MAOI**	**Control**	***F***	**partial η^2**
1.) Spontaneous locomotor activity					
Immediately following drug treatment	41.9% ± 30.6_a n = 62	17.8% ± 24.1_b n = 59	30.5% ± 25.2_c n = 45	10.326*	.112
Repeated measures					
1 hour post treatment (Group)	53.8% ± 25.7_a n = 20	3.7% ± 6.2_b n = 13	55.6% ± 32.8_a n = 25	20.925*	.482
24 hours post treatment (Time)	8.6% ± 15.1_a n = 20	3.8% ± 6.8_b n = 13	21.8% ± 26.4_c n = 25	40.655*	.475
Time x Group interaction				11.920*	.346
2.) Visually-evoked startle response					
Overall response probability	80.9% ± 37.1_a n = 21	33.3% ± 37.2_b n = 15	95.8% ± 37.0_a n = 12	24.658*	.523
Repeated measures					
Latency (mS) 1 hour post treatment (Group)	188 ± 58_a n = 21	N/A	140 ± 55_a n = 12	1.309	.068
Latency (mS) 24 hours post treatment (Time)	346 ± 93_a n = 21	N/A	315 ± 164_a n = 12	31.731*	.638
Time x Group interaction				.103	.006

Subscripts indicate homogenous subsets as determined by a Tukey's-b or simple effects test. F statistics marked with an asterisk indicate statistical significance at $p < .05$.

Dopaminergic cells

Pretectal cell populations. The number of DAT-expressing cells in the pretectum of 7 dpf zebrafish larvae was influenced by drug exposure, $F(2,55) = 4.316$, $p = .018$, partial $\eta^2 = .136$ (Table 3, Figure 8). Control fish ($n = 25$) had 59.4 cells on average. L-DOPA treated fish ($n = 20$) had the greatest reduction in cell numbers, with a mean of 51.3, while MAOI treated fish ($n = 13$) exhibited an intermediate mean of 54.9 (Figure 10).

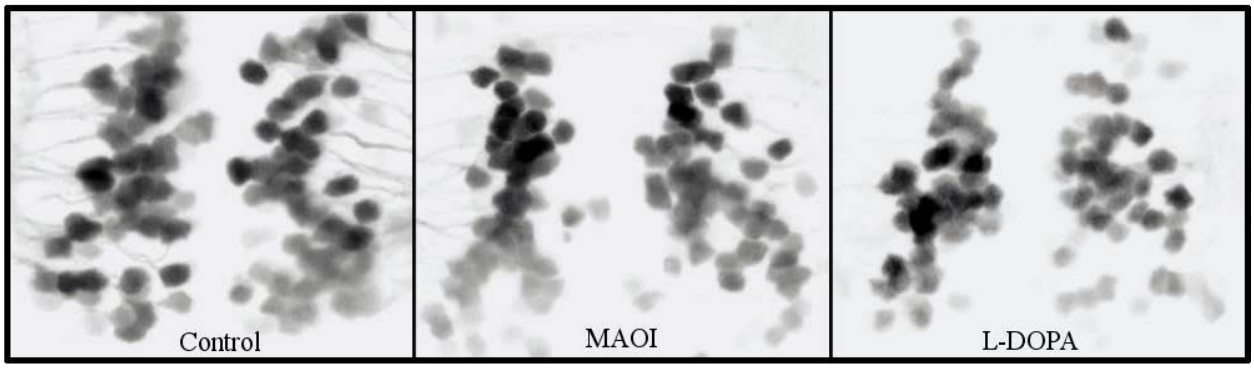

Figure 8. 3X optical zoom images of fluorescent DAT-expressing pretectal cells from each group in 7 dpf zebrafish larvae following drug treatment. Images were not manipulated and background intensity is matched across the images presented. Images acquired by Sarah Stednitz.

vDC fluorescence intensity. To ensure the results obtained from pretectal cell counts were not a result of preexisting differences between groups, a repeated measures experiment was implemented to examine changes in fluorescence intensity in the vDC due to drug treatment within animals. Main effects for time and group on fluorescence were observed, $F(1,40) = 11.420$, $p = .002$, partial $\eta^2 = .222$ and $F(2,40) = 5.580$, $p = .007$, partial $\eta^2 = .218$. There was also an interaction between treatment group and time, $F(2,40) = 4.119$, $p = .024$, partial $\eta^2 = .149$ (Figure 10). Groups did not differ from one another at the initial 4 dpf measurement time, $F(2,40) = 0.924$, $p = .405$, partial $\eta^2 = .044$. Following drug treatment, control and MAOI groups

had significant increases in fluorescence intensity of 24.3% and 32.3% respectively ($F(1,40) = 6.673$, $p = .014$ and $F(1,40) = 9.881$, $p = .003$). In contrast, the L-DOPA group exhibited an average increase of only 1.5%, $F(1,40) = .048$, $p = .827$ (Figure 9, Table 3).

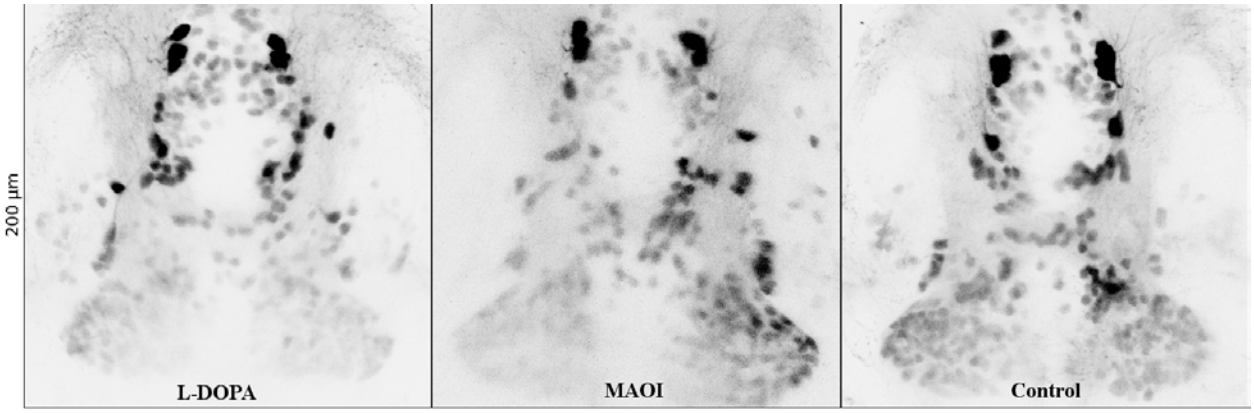

Figure 9. 2X optical zoom images of fluorescent DAT-expressing vDC cells from each group in 5 dpf zebrafish larvae following drug treatment. Images were not manipulated and background intensity is matched across the images presented. Images acquired by Sarah Stednitz.

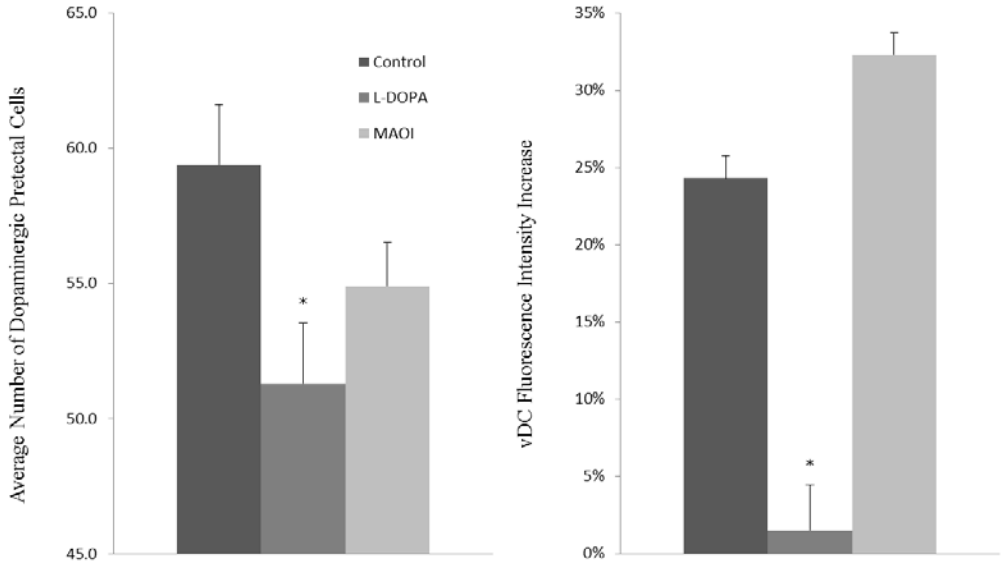

Figure 10. Left: Average number of dopaminergic pretectal cells in 7 dpf larvae following 24 hour drug treatment. Right: Average increase in vDC fluorescence intensity following 24 hour drug treatment in 4 and 5 dpf larvae. Error bars indicate s.e.m., and asterisks indicate groups that differ significantly from the control.

Table 3.
Means, standard deviations, and statistical tests for all imaging experiments performed.

Experiment	L-DOPA	L-DOPA & MAOI	Control	F	partial η^2
1.) Pretectal cell numbers	$51.3 \pm 7.3_a$ $n = 20$	$54.9 \pm 8.1_{a,b}$ $n = 13$	$59.4 \pm 11.0_b$ $n = 25$	4.316*	.136
2.) Change in vDC fluorescence intensity	$1.5\% \pm 6.2_a$ $n = 19$	$32.3\% \pm 8.9_b$ $n = 9$	$24.3\% \pm 6.5_b$ $n = 15$	11.420*	.222

Subscripts indicate homogenous subsets as determined by a Tukey's-b test. F statistics marked with an asterisk indicate statistical significance at $p < .05$.

Discussion

The results of these experiments indicate that the product of dopamine's metabolism by MAO may be toxic to DA neurons, and administration of drugs that inhibit this metabolism may protect against dopaminergic cell loss in Parkinson's disease and related conditions. Reductions in DAT-expressing neuron populations were observed in both the vDC and the pretectum after L-DOPA treatment. This agrees with previous studies showing that the dopaminergic cells of the vDC are vulnerable in zebrafish models of PD, possibly due to their expression of the DAT (McKinley et al., 2005; Lam, Korzh, & Strahle, 2005; Xi et al., 2011).

The initial behavioral hyperactivity observed after treatment with L-DOPA is consistent with previous reports on behavioral responses to dopaminergic agents in zebrafish larvae and other animals (Irons, MacPhail, Hunter, & Padilla, 2010). Drugs of abuse that augment dopamine transmission, such as cocaine and amphetamines, have long been associated with hyperactive behaviors (O'Neill & Shaw, 1999). Conversely, dopamine receptor antagonists such as haloperidol or similar antipsychotics abolish these behaviors and cause locomotor depression. These effects are related to the major dopaminergic projections in the brain, including the nigrostriatal pathway affected in PD. In contrast to the initial hyperactivity, locomotor behavior was depressed when tested 24 hours after L-DOPA washout. This is consistent with the observed cell loss described in this study and with previous research reporting dopaminergic cell loss and locomotor inhibition in zebrafish models of PD. In concordance with the current understanding of PD etiology, the loss of dopamine producing cells causes disruptions to motor behaviors due to reduced neurotransmitter signaling. Research with zebrafish larvae has confirmed that dopaminergic cells are required for motor function and their loss results in behavioral deficits

(Anichtchik et al., 2008; Flinn et al., 2009; Lam et al., 2005; McKinley et al., 2005; Xi et al., 2010; Xi et al., 2011). These acute and delayed drug effects reinforce the importance of dopamine signaling to locomotor behavior in zebrafish larvae, and vertebrate animals in general.

In contrast to spontaneous swimming bouts, visually-evoked startle response rates and latencies were unaffected by L-DOPA treatment. This finding supports the use of the startle response as a negative control in studies of spontaneous activity in zebrafish. The startle response rate was substantially diminished in MAOI-treated larvae. The MAOI was used in this study to counteract the neurotoxic effects of L-DOPA, but it is also a direct modulator of serotonin levels, which may explain the startle inhibition observed here. Because so few startles responses occurred in the MAOI treated larvae it was not possible to measure response latencies in those groups. Zebrafish possess only one isoform of MAO, and as a result MAO-B inhibitors have broader effects in zebrafish than in mammals, including elevated serotonin concentrations (Anichtchik, Sallinen, Peitsaro & Panula, 2006). MAOI treated larvae had a reduced survival rate during the imaging process compared to L-DOPA or control animals, possibly due to decreased blood flow. Serotonin signaling has also been implicated in arousal (Yokogawa, Hannan, & Burgess, 2012) in zebrafish larvae, potentially disrupting startle responsiveness. Reticulospinal neurons that mediate the startle response also show evidence of modulation by serotonin (McLean & Fetcho, 2004), potentially confounding any effect from dopamine cell loss.

Extracellular oxidative stress caused by the formation of autoxidative products remains a possible mechanism for cell death, although prior research on methamphetamine-induced neurotoxicity suggests that augmented extracellular dopamine is insufficient to cause lesions (LaVoie & Hastings, 1999). Repetition of this experiment with zebrafish knockdowns of PD-

associated genes, such as *PINK1*, would lend further support to the relevance of dopamine toxicity to PD. The oxidative stress hypothesis suggests that these larvae should have a compromised ability to cope with dopamine toxicity, and an increased vulnerability to neurotoxic insults. Western blots for protein carbonylation, a marker of oxidative stress, could indicate if DAT cells are selectively susceptible to oxidation caused by L-DOPA treatment. Future experiments with the Oxyblot protein carbonylation kit are planned, and this protein analysis may also provide evidence that MAOIs act to reduce oxidative stress in the affected cells.

In addition to the need for direct measurement of oxidative stress after drug treatments, the current experiments would have benefited from measurements of DOPAL and DOPAC. While direct administration of DOPAL would have provided stronger evidence of its neurotoxic properties, its instability in solution makes administration in larval zebrafish more difficult than in mammalian models. In addition, given that non-dopaminergic cell populations were not observed in the current study, it is not possible to definitively conclude that DAT neurons alone are affected and future research would benefit from the inclusion of a control population of non-DAT cells.

Despite these shortcomings, the results of the current study lend support to the emerging use of MAOIs as a monotherapy in PD, a treatment that is currently receiving considerable interest in clinical trials. This treatment approach will depend on early diagnosis because the strategy is to prevent dopaminergic neuron loss, and this has already occurred by later stages. The most successful clinical trial of MAOI therapy to date focused on early diagnosed patients for this reason (Rascol et al, 2011). Unfortunately, until presymptomatic diagnosis of PD is

possible, there may be no way to directly translate these animal models of preventative drug therapy into human treatments.

Further research would benefit from blocking the DAT to determine if these effects are replicable when access to the intracellular space is prevented. Laser ablation of individual dopaminergic neurons, using GFP expression to target the laser, could compliment studies using dopaminergic toxins to gain a better understanding of the consequences of dopamine cell loss. Using additional behavioral measurements in these experiments would also help define the function of the dopaminergic system in zebrafish. For instance, the tectum is required for visually-guided prey capture in zebrafish larvae (Gahtan, Tanger, & Baier, 2005), and this behavior could be used to demonstrate more subtle effects of dopamine disruption on visual processing and motor control. Ultimately, experiments that bridge the gap between pharmacological models of dopamine neurotoxicity and genetic models of PD should yield the most clinically relevant results.

References

Anichtchik, O., Deikmann, H., Fleming, A., Roach, A., Goldsmith, P., & Rubinsztein, D. C. (2008) Loss of PINK1 function affects development and results in neurodegeneration in zebrafish. *Journal of Neuroscience*, *28*, 8199-8207. doi:10.1523/jneurosci.0979-08.2008

Anichtchik, O., Sallinen, V., Peitsaro, N., & Panula, P. (2006) Distinct structure and activity of monoamine oxidase in the brain of zebrafish (*Danio rerio*). *Journal of Comparative Neurology*, *498*, 593-610. doi:10.1002/cne.21057

Bronstein, J. M., Tagliati, M., Alterman, R. L., Lozano, A. M., Volkman, J., Stefani, A., ... DeLong, M. R. (2011) Deep brain stimulation for Parkinson disease. *Archives of Neurology*, *68*, 165. doi:10.1001/archneurol.2010.260

Burke, W. J., Li, S. W., Chung, H. D., Ruggiero, D. A., Kristal, B. S., Johnson, E. M., ... Zahm, D.S. (2004) Neurotoxicity of MAO metabolites of catecholamine neurotransmitters: role in neurodegenerative diseases. *Neurotoxicology*, *25*, 101-115. doi: 10.1016/S0161-813X(03)00090-1

Castagnoli, K., & Murugesan, T. (2004) Tobacco leaf, smoke and smoking, MAO inhibitors, Parkinson's disease and neuroprotection; are there links? *Neurotoxicology*, *25*, 279-91. doi:10.1016/S0161-813X(03)00107-4

de Lau, L. M., & Breteler, M. M. (2006) Epidemiology of Parkinson’s disease. *Lancet Neurology*, *5*, 525-35. doi:10.1016/S1474-4422(06)70471-9

Fearnley, J. M., & Lees, A. J. (1991) Ageing and Parkinson’s disease: Substantia nigra regional selectivity. *Brain*, *114*, 2283-2301. doi:10.1093/brain/114.5.2283

Flinn, L., Mortiboys, H., Volkmann, K., Koster, R. W., Ingham, P. W., & Bandmann, O. (2009) Complex I deficiency and dopaminergic neuronal cell loss in parkin-deficient zebrafish (Danio rerio). *Brain*, *132*, 1613-1623. doi: 10.1093/brain/awp108

Fowler, J. S., Volkow, N. D., Wang, G. J., Logan, J., Pappas, N., Shea, C., & MacGregor, R. (1997) Age-related increases in brain monoamine oxidase B in living healthy human subjects. *Neurobiology of Aging*, *18*, 431-435. doi:10.1016/S0197-4580(97)00037-7

Fowler, J. S., Volkow, N. D., Wang, G. J., Pappas, N., Logan, J., Macgregor, R., ... Zezulkova, I. (1998) Brain monoamine oxidase (MAO B) inhibition. *Journal of Addictive Diseases, 17*, 23-34. doi: 10.1300/J069v17n01_03

Gahtan, E., Tanger, P., & Baier, H. (2005) Visual prey capture in larval zebrafish is controlled by identified reticulospinal neurons downstream of the tectum. *Journal of Neuroscience, 25*, 9294-9303. doi:10.1523/jneurosci.2678-05.2005

Goldstein, D. S., Sullivan, P., Holmes, C., Kopin, I. J., Basile, M. J., & Mash, D. C. (2011) Catechols in post-mortem brain of patients with Parkinson disease. *European Journal of Neurology*, *18*, 703-710. doi:10.1111/j.1468-1331.2010.03246.x

Goldstein, D. S., Sullivan, P., Holmes, C., Miller, G. W., Alter, S., Strong, R., . . Sharabi, Y. (2013) Determinants of buildup of the toxic dopamine metabolite DOPAL in Parkinson's disease. *Journal of Neurochemistry*, *126*, 591-603. doi:10.1111/jnc.12345

Groenewegen, H. J. (2003) The basal ganglia and motor control. *Neural Plasticity*, *10*, 107-120. doi:10.1155/NP.2003.107

Irons, T. D., MacPhail, R.C., Hunter, D. L., & Padilla, S. (2010) Acute neuroactive drug exposures alter locomotor activity in larval zebrafish. *Neurotoxicology and Teratology*, *32*, 84-90.

Kimmel, C. B., Patterson, J., & Kimmel, R. O. (1974) The development and behavioral characteristics of the startle response in the zebra fish. *Developmental Psychobiology, 7*, 47-60. doi:10.1242/jeb.01534

Kitada, T., Asakawa, S., Hattori, N., Matsumine, H., Yamamura, Y., Minoshima, . . Shimizu, N. (1998) Mutations in the *parkin* gene cause autosomal recessive juvenile parkinsonism. *Nature*, *392*, 605-608. doi:10.1038/33416

Lam, C. S., Korzh, V., & Strahle, U. (2005) Zebrafish embryos are susceptible to the dopaminergic neurotoxin MPTP. *European Journal of Neuroscience*, *21*, 1758-1762. doi:10.1111/j.1460-9568.2005.03988.x

Langston, J. W., & Palfreman, J. (1996) The Case of the Frozen Addicts: How the solution of an extraordinary medical mystery spawned a revolution in the understanding and treatment of Parkinson's disease. New York, NY: Pantheon. doi:10.1056/nejm199612263352618

LaVoie, M. J., & Hastings, T. G. (1999) Dopamine quinone formation and protein modification associated with the striatal neurotoxicity of methamphetamine: evidence against a role for extracellular dopamine. *Journal of Neuroscience, 19*, 1484-1491. doi:10.1046/j.1471-4159.2001.00339.x

Li, S. W., Lin, T., Minteer, S., & Burke, W. J. (2001) 3-4-Dihydroxyphenylacetaldehyde and hydrogen peroxide generate a hydroxyl radical: possible role in Parkinson's disease pathogenesis. *Molecular Brain Research*, *93*, 1-7. doi:10.1111/j.1471-4159.2012.07924.x

McKinley, E. T., Baranowski, T. C., Blavo, D. O., Cato, C., Doan, T. N., & Rubinstein, A. L. (2005) Neuroprotection of MPTP-induced toxicity in zebrafish dopaminergic neurons. *Molecular Brain Research, 141,* 128-37. doi:0.1016/j.molbrainres.2005.08.014

McLean, D. L., & Fetcho, J.R. (2004) Relationship of tyrosine hydroxylase and serotonin immunoreactivty to sensorimotor circuitry in larval zebrafish. *Journal of Comparative Neurology*, *480*, 57-71. doi:10.1002/cne.20281

McQueen, C. A. (Ed.) (2010) Comprehensive Toxicology. Amsterdam, North Holland: Elsevier Science, p. 423.

Merims, D., & Giladi, N. (2008) Dopamine dysregulation syndrome, addiction and behavioral changes in Parkinson's disease. *Parkinsonism and Related Disorders*, *14*, 273-280. doi:10.1016/j.parkreldis.2007.09.007

Muto, A., Orger, M. B., Wehman, A. M., Smear, M. C., Kay, J. N., Page-McCaw, P. S., ... Baier, H. (2005) Forward genetic analysis of visual behavior in zebrafish. PLoS Genetics, 1(5):e66. doi:10.1371/journal.pgen.0010066

Olanow, C. W., Rascol, O., Hauser, R., Feigin, P. D., Jankovic, J., Lang, A., ... Tolosoa, E. (2009) A double-blind, delayed-start trial of rasagiline in Parkinson's disease. *New England Journal of Medicine, 361,* 12688-1278. doi:10.1056/nejmoa0809335

O'Neill, M. F., & Shaw, G. (1999) Comparison of dopamine receptor antagonists on hyperlocomotion induced by cocaine, amphetamine, MK-801 and the dopamine D1 agonist C-APB in mice. P*sychopharmacology*, *145*, 237-250. doi:10.1007/s002130051055

Parkinson Study Group (2005). A randomized placebo-controlled trial of rasagiline in levodopa-treated patients with Parkinson disease and motor fluctuations: the PRESTO study. *Archives of Neurology, 62*, 241-248. doi:10.1001/archneur.62.2.241

Panneton, W. M., Kumar, V. B., Gan, Q., Burke, W. J., & Galvin, J. E. (2010) The neurotoxicity of DOPAL: behavioral and stereological evidence for its role in Parkinson disease pathogenesis. *PLoS One*, *5*(12):e15251. doi:10.1371/journal.pone.0015251

Portugues, R., & Engert, F. (2009) The neural basis of visual behaviors in the larval zebrafish. *Current Opinion in Neurobiology*, *19*, 1-4. doi:10.1016/j.conb.2009.10.007

Pridgeon, J. W., Olzmann, J. A., Chin, L. S., & Li, L. (2007) PINK1 protects against oxidative stress by phosphorylating mitochondrial chaperone TRAP1. *PLoS Biology, 5*(7), e172. doi:10.1371/journal.pbio.0050172

Rascol, O., Brooks, D. J., Melamed, E., Oertel, W., Poewe, W., Stocchi, F., & Tolosa, E. (2005) Rasagiline as an adjunct to levodopa in patients with Parkinson's disease and motor fluctuations (LARGO, Lasting effect in Adjunct therapy with Rasagiline Given Once daily, study): A randomized, double-blind, parallel-group trial. *The Lancet, 365*, 947-954. doi:10.1016/j.parkreldis.2013.06.001

Rascol, O., Fitzer-Atlas, C. J., Hauser, R., Jankovic, J., Lang, A., Langston, J.W., ... Olanow, C.W. (2011) A double-blind, delayed-start trial of rasagiline in Parkinson's disease (the ADAGIO study): prespecified and post-hoc analyses of the need for additional therapies, changes in UPDRS scores, and non-motor outcomes. *Lancet Neurology, 10*, 415-423. doi:10.1016/S1474-4422(11)70073-4

Sallinen, V., Sundvik, M., Reenilä, I., Peitsaro, N., Khrustalyov, D., Anichtchik, O., Toleikyte, G., Kaslin, J., & Panula, P. (2009) Hyperserotonergic phenotype after monoamine oxidase inhibition in larval zebrafish. *Journal of Neurochemistry*, *109*, 403-415. doi:10.1111/j.1471-4159.2009.05986.x

Saura, J., Andres, N., Andrade, C., Ojuel, J., Eriksson, K., & Mahy, N. (1997) Biphasic and region-specific MAO-B response to aging in normal human brain. *Neurobiology of Aging*, *18*, 497-507. doi:10.1016/S0197-4580(97)00113-9

Schweitzer, J., Heiko, L., Filippi, A., & Driever, W. (2012) Dopaminergic and noradrenergic circuit development in zebrafish. *Developmental Neurobiology, 72*, 256-268. doi:10.1002/dneu.20911.

Selderslaghs, I. W., Hooyberghs, J., De Coen, W., & Witters, H. E. (2010) Locomotor activity in zebrafish embryos: a new method to assess developmental neurotoxicity. *Neurotoxicology & Teratology*, *32*, 460-471. doi:10.1016/j.ntt.2010.03.002

Tay, T. L., Ronneberger, O., Ryu, S., Nitschke, R., & Driever, W. (2011) Comprehensive catecholaminergic projectome analysis reveals single-neuron integration of zebrafish ascending and descending dopaminergic systems. *Nature Communications*, *2*, doi:10.1038/ncomms1171.

Xi, Y., Ryan, J., Noble, S., Yu, M., Yilbas, A. E., & Ekker, M. (2010) Impaired dopaminergic neuron development and locomotor function in zebrafish with loss of pink1 function. *European Journal of Neuroscience, 31*, 623-33. doi:10.1111/j.1460-9568.2010.07091.x

Xi, Y., Yu, M., Godoy, R., Hatch, G., Poitras, L., & Ekker, M. (2011). Transgenic zebrafish expressing green fluorescent protein in dopaminergic neurons of the ventral diencephalon. *Developmental Dynamics, 240*, 2539-2547. doi:10.1002/dvdy.22742

Yokogawa, T., Hannan, M. C., & Burgess, H. A. (2012) The dorsal raphe modulates sensory responsiveness during arousal in zebrafish. *Journal of Neuroscience*, *32,* 15205-15215. doi:10.1523/jneurosci.1019-12.2012

Appendix A

Script - ImageJ

```
//ImageJ script for analysis of zebrafish locomotor behavior in multiwell plates
//Gahtan Lab - Written by Sarah Stednitz, Briana Freshner, Kendra Hartsuyker
//Works on ImageJ 1.47a Java 1.6.0_27 32-bit Ubuntu 13.04
//Files must be separated into numbered folders manually or via BASH script
//Rois defined and saved in advance, named by column (A, B, C) and row (1, 2, 3)
//This example script uses a 24 well plate with 6 recording epochs.
//*******SET IMAGE THRESHOLD AT LINE 87********
//MANUAL FILE DEFINITIONS
//Define number of folders to be processed
foldercount=6;
//Define directory paths for images, rois, and results - make sure these exist
directory="C:/data/date/";
roifolder="C:/data/date/rois/";
resultsdir="C:/data/date/results”;
//number of images to load per folder
numimages = "300";
//define column labels, number of columns, and rows per column.
columnarray=newArray('A','B','C','D'); /*column labels, check case, make sure there
are rois for each column, don't add columns that don't exist*/
rownumbers=6;
columnnumbers=4;

//initialize folder counter & id variable
foldernum=0;
idvar=0;
wellcoordinates='';

//calculate variables based on manual definitions
wellnum=(rownumbers*columnnumbers)-1;
greyarray=newArray(foldercount*rownumbers*columnnumbers);
roiname=newArray(rownumbers*columnnumbers);
rownumbersplus1=rownumbers+1;

//load ROIs to be used later
for (n=0; n<columnnumbers; n++){
    for (o=1; o<rownumbersplus1; o++){
        wellcoordinates = columnarray[n] + o;
        roiname = wellcoordinates;
        roiManager("Open", roifolder+wellcoordinates+".roi");
    }
}

//Loop starts here
for (j=0; j<foldercount; j++) {
    //Add to active folder #
    foldernum=foldernum + 1;
    //Print to window so you can check which folder it's on at any given time
```

```
    print("Processing folder "+foldernum);
    //Define directory to search for folders - MAKE SURE THIS PATH IS CORRECT!
    dir=directory+foldernum;
    //Concatenate directory path sequentially to avoid bug w/ interpreting numerical
vs string input
    arg = "open=" + dir;
    arg = arg + "/*.jpg number="+numimages+" starting=1 increment=1 scale=100";
    //Import image sequence using previously defined argument
    run("Image Sequence...", arg);
//~~~~IMAGE PROCESSING GOES HERE~~~~
//Use batch mode to speed things up; disable if you need to see the images
    setBatchMode(true);
    //Add inverted images at beginning to force particle detection results even if
fish does not move
    run("Add Slice");
    run("Add Slice");
    run("Invert", "slice");
    //Successive subtraction to isolate only pixels that have changed
    run("8-bit");
    setPasteMode("Subtract");

    for(i=1; i<nSlices; i++){
        run("Next Slice [>]");
         }
    for(i=1; i<nSlices; i++){
             run("Previous Slice [<]");
             run("Select All");
             run("Copy");
             run("Next Slice [>]");
             run("Paste");
             run("Previous Slice [<]");
         }
    run("Delete Slice", "");
//******SET THRESHOLD******
//Threshold successive subtraction sequence after selecting the correct window.
//Particle analysis requires a binarized (thresholded) image to work.
//Manually determine appropriate threshold in ImageJ before running script.
    selectWindow(directory+foldernum);
    setThreshold(22, 255);
 //Perform particle analysis for each ROI, save results to text in results dir
 //Change the q<56 bit to however many wells we're looking at.
    for (p=0; p<columnnumbers; p++){
            for (r=0; r<rownumbers; r++){
            wellcoordinates = columnarray[p] + r;
            roiManager("Select", idvar);
            run("Analyze Particles...", "size=3-Infinity circularity=0.00-1.00
show=Nothing clear summarize stack");
            selectWindow("Summary of "+directory+foldernum);
            idvar=idvar+1;
            saveAs("Text", resultsdir+foldernum+wellcoordinates+"Summary.txt");
            run("Close");
//~~~~END IMAGE PROCESSING~~~~
            }
```

```
    }
    idvar = 0; /* reset idvar to 0 to start from begining in new folder */
    //Close remaining windows
    selectWindow(directory+foldernum);
    run("Close");
}
```

Script - R

```
# 1-way or repeated measures code--change foldernum to switch between
framework <- read.table("/home/zflab/Dropbox/thesis/R-automation/framework.csv",
 header=TRUE, sep=",", na.strings="NA", dec=".", strip.white=TRUE)
framework$group <- factor(framework$group)
#set number of images in each recording period to calculate avg
imagenum = 300
#for one-way, use foldernum = 1
foldernum = 1
#define directory to look for data
string1="/home/zflab/Dropbox/thesis/3-14-spontact/"

#set null variables for use later
id_var = NULL
framework$avg = NULL
temprows = NULL

library(reshape)
library(ez)

if (foldernum == 1){
       for (i in 1:nrow(framework)) {
              #LOOP THIS adding to framework$id[i] until == to nrow(framework)
              id_var = framework$id[i]
              string2="Summary.txt"
              string3<-paste(string1,foldernum,id_var,string2,sep="")
              temp <- read.table(string3, header=TRUE, sep="",
                     na.strings="NA", dec=".", strip.white=TRUE)
              temprows <- (length(unique(temp$Label)))
              framework$avg[i] = (temprows/imagenum)
              #END LOOP
       }

       framework <-as.data.frame(framework)
       ANOVAResults <- aov(avg~group, data=framework)
       print("Means")
       tapply(framework$avg, list(group=framework$group), mean, na.rm=TRUE)
       print("Standard Deviations")
       tapply(framework$avg, list(group=framework$group), sd, na.rm=TRUE)
       summary(ANOVAResults)
       TukeyHSD(ANOVAResults)
} else {
       totalrows = (nrow(framework))*foldernum
       RMframework <-matrix(0, ncol = 4, nrow = totalrows)
```

```
	RMframework <- as.data.frame(RMframework)

	id_var = NULL

	RMframework <- rename(RMframework, c(V1="id", V2="group", V3="avg",
V4="trial"))
	temprows = NULL
	RMrows = 1


	for (i in 1:nrow(framework)) {
		for (k in 1:foldernum){
			id_var = framework$id[i]
			string2="Summary.txt"
			string3<-paste(string1,k,id_var,string2,sep="")
			temp <- read.table(string3, header=TRUE, sep="",
				na.strings="NA", dec=".", strip.white=TRUE)

			RMframework$group[RMrows] = framework$group[i]
			RMframework$id[RMrows] = framework$id[i]
			RMframework$trial[RMrows] = k

			temprows <- length(unique(temp$Label))
			RMframework$avg[RMrows] = (temprows/imagenum)

			RMrows = RMrows + 1
		}
	}
	RMframework$group <-factor(RMframework$group)
	RMframework$trial <-factor(RMframework$trial)

	#Means
	tapply(RMframework$avg, list(group=RMframework$group), mean, na.rm=TRUE)
	tapply(RMframework$avg, list(group=RMframework$trial), mean, na.rm=TRUE)
	ezANOVA(data=RMframework, dv=.(avg), wid=.(id), between=.(group),
within=.(trial),detailed=TRUE,type="III")
}
```